



Exosomal CircPRRX1 Enhances Doxorubicin Resistance in Gastric Cancer by Regulating MiR-3064-5p/PTPN14 Signaling

Shumin Wang, Mei Ping, Bin Song, Yarong Guo, Yuanfei Li, and Junmei Jia

Department of Oncology, First Hospital of Shanxi Medical University, Taiyuan City, Shanxi Province, China.

Purpose: Gastric cancer (GC) is a malignant tumor with a high mortality rate. Drug resistance is a major obstacle to GC therapy. This study aimed to investigate the role and mechanism of exosomal circPRRX1 in doxorubicin resistance in GC.

Materials and Methods: HGC-27 and AGS cells were exposed to different doses of doxorubicin to construct doxorubicin-resistant cell lines. Levels of circPRRX1, miR-3064-5p, and nonreceptor tyrosine phosphatase 14 (PTPN14) were detected by quantitative real-time PCR or Western blot assay. Then, 3-(4,5-dimethyl-2-thiazolyl)-2,5-diphenyl-2-H-tetrazolium bromide, transwell, and Western blot assays were used to explore the function of circPRRX1 in GC cells. Interactions among circPRRX1, miR-3064-5p, and PTPN14 were confirmed by dual-luciferase reporter assay. The in vivo function of circPRRX1 was analyzed in a xenograft tumor model.

Results: CircPRRX1 was highly expressed in doxorubicin-resistant GC cell lines. Knockdown of circPRRX1 reversed doxorubicin resistance in doxorubicin-resistant GC cells. Additionally, extracellular circPRRX1 was carried by exosomes to spread doxorubicin resistance. CircPRRX1 silencing reduced doxorubicin resistance by targeting miR-3064-5p or regulating PTPN14. In GC patients, high levels of circPRRX1 in serum exosomes were associated with poor responses to doxorubicin treatment. Moreover, depletion of circPRRX1 reduced doxorubicin resistance in vivo.

Conclusion: CircPRRX1 strengthened doxorubicin resistance by modulating miR-3064-5p/PTPN14 signaling and might be a therapeutic target for GC patients.

Key words: Gastric cancer, CircPRRX1, MiR-3064-5p, PTPN14, Exosome, Doxorubicin

INTRODUCTION

Gastric cancer (GC) is a common gastrointestinal cancer that ranks third in cancer-related deaths.¹ The occurrence of GC is primarily caused by *Helicobacter pylori* infections.² Due to the emergence of drug resistance, conventional chemotherapy

strategies have limited efficacy in patients with advanced GC.³ Therefore, exploring the molecular mechanism of GC resistance is crucial to improving the prognosis of GC.

Recently, accumulating evidence has indicated that circular RNAs (circRNAs) with covalent closed-loop structures exert a vital regulatory effect on the occurrence and development of various cancers.⁴ Abnormally expressed circRNAs in GC have been found to mediate tumor progression by regulating microRNAs:⁵ for example, circ-RanGAP1 accelerated tumor metastasis in GC through a miR-877-3p/VEGFA regulatory axis.⁶ Circ-PVT1 enhanced the resistance of GC cells to paclitaxel via down-regulating miR-124-3p and elevating ZEB1.⁷ Also, circFN1 targeted miR-182-5p to regulate cisplatin sensitivity in GC.⁸ Furthermore, high-throughput sequencing results have revealed that hsa_circ_0004370 derived from paired-related homeobox 1 (PRRX1) is up-regulated in GC tissues. However, the function of circPRRX1 in GC progression has

Received: March 26, 2020 **Revised:** June 16, 2020

Accepted: June 22, 2020

Corresponding author: Junmei Jia, MM, Department of Oncology, First Hospital of Shanxi Medical University, No. 85 South Jiefang Road, Yingze District, Taiyuan City, 030001, Shanxi Province, China.

Tel: 86-139-34249371, Fax: 86-0351-4048624, E-mail: iniawj@163.com

•The authors have no potential conflicts of interest to disclose.

© Copyright: Yonsei University College of Medicine 2020

This is an Open Access article distributed under the terms of the Creative Commons Attribution Non-Commercial License (<https://creativecommons.org/licenses/by-nc/4.0>) which permits unrestricted non-commercial use, distribution, and reproduction in any medium, provided the original work is properly cited.

not been investigated.

Emerging evidence has demonstrated that circRNAs can modulate gene expression through competing endogenous RNA (ceRNA) mechanisms or by serving as miRNA sponges.⁹ In our preliminary research, bioinformatics software indicated that circPRRX1 might be a decoy for miR-3064-5p. Hence, we investigated the relationship between circPRRX1 and miR-3064-5p in doxorubicin resistance among GC cells. Meanwhile, nonreceptor tyrosine phosphatase 14 (PTPN14) has been identified as a potential tumor suppressor by interacting with YAP, a key effector of the Hippo signaling pathway:¹⁰ for instance, PTPN14 has been found to suppress osteosarcoma development via deactivating YAP1.¹¹ However, one previous study showed that PTPN14 is a tumor-promoting factor in GC, inducing epithelial-to-mesenchymal transition (EMT).¹²

Exosomes are nanovesicles that contain a large number of functional biomolecules.¹³ Exosome-encapsulated biomolecules participate in intercellular communication by being absorbed by other cells.¹⁴ Exosomal circRNAs contribute to tumor metastasis and cell communication by influencing the biological processes of recipient cells.¹⁵ Whether exosomes secreted by resistant cancer cells can confer chemoresistance to sensitive cells, however, is largely unknown. Therefore, we explored the effect of exosome-mediated circRNA on doxorubicin resistance.

In the present study, we explored the effect of exosome-mediated circPRRX1 on doxorubicin resistance and tumor progression. Furthermore, the therapeutic significance of exosomal circPRRX1 in doxorubicin-resistant GC patients was investigated.

MATERIALS AND METHODS

Clinical specimens

This research was ratified by the Ethics Committee of First Hospital of Shanxi Medical University. Fifty-six GC patients who received doxorubicin treatment were recruited from First Hospital of Shanxi Medical University. From each participant, 5 mL of venous blood was collected using venipuncture, and serum samples were obtained by centrifugation. The clinicopathologic features of these patients are presented in Table 1. All participants signed written informed consent. According to the Response Evaluation Criteria in Solid Tumors, GC patients were divided into response (n=24) and non-response (n=32) groups.

Cell culture

Human GC cell lines (HGC-27 and AGS) were obtained from Shanghai Honsun Biotechnology Co., Ltd (Shanghai, China). HGC-27 and AGS cells were exposed to increasing doses of doxorubicin (DR; Solarbio, Beijing, China) to generate doxorubicin-resistant GC cell lines (HGC-27/DR and AGS/DR). The resistant cells were incubated with doxorubicin (1 µg/mL). All cells were

Table 1. Clinicopathological features of the patients (n=56)

Sex	
Female	35
Male	21
Age (yr)	
≥60	36
<60	20
Tumor size (cm)	
≥3	24
<3	32
Tumor site	
Cardiac	34
Non-cardiac	22
<i>Helicobacter pylori</i> infection	
Yes	27
No	29
TNM stage	
I-II	23
III-IV	33

cultured in RPMI-1640 medium (Gibco, Carlsbad, CA, USA) supplemented with 10% fetal bovine serum (FBS; Gibco) at 37°C with 5% CO₂.

Exosome isolation

In brief, the culture medium of doxorubicin-resistant cells and serum were centrifuged at 3000×g for 10 min to precipitate cells and then centrifuged at 10000×g for 30 min to remove cell debris. Then, the supernatant was ultracentrifuged at 110,000×g for 60 min, and the exosomes were resuspended in PBS, followed by ultracentrifugation for 60 min to purify exosomes. Additionally, a Philips CM120 transmission electron microscope (TEM) (Philips Research, Eindhoven, Netherlands) was used to observe the morphology of exosomes.

Cell transfection

Small interfering RNA (siRNA) against circPRRX1 (si-circPRRX1), siRNA control (si-NC), miR-3064-5p mimics (miR-3064-5p), mimics control (miR-NC), miR-3064-5p inhibitor (anti-miR-3064-5p), inhibitor control (anti-miR-NC), PTPN14 overexpression vector (PTPN14), and empty overexpression vector (vector) were purchased from GenePharma (Shanghai, China). Lipofectamine 3000 (Invitrogen, Carlsbad, CA, USA) was used to transfect oligonucleotides or vectors into cells.

Quantitative real-time PCR (qRT-PCR)

Total RNA was extracted using TRIzol reagent (Invitrogen). The complementary DNA was synthesized using the FastQuant RT Kit (Tiangen, Beijing, China) or miScript II RT Kit (Qiagen, Frankfurt, Germany). Expression levels were detected using AceQ qPCR SYBR Green Master Mix (Vazyme, Nanjing, China) and calculated using 2^{-ΔΔCt} method. GAPDH or U6 was used as

an internal control. Primers were as follows: circPRRX1-F: 5'-ACCCACCGATTATCTCTCCTG-3'; circPRRX1-R: 5'-TCCTATTCCTTCGCTGCTTTC-3'; miR-3064-5p-F: 5'-CTG-GCTGTTGTGGTGTGC-3'; miR-3064-5p-R: 5'-TGGTGTCTGTG-GAGTCG-3'; PTPN14-F: 5'-ATGCCTTTTGGTCTGAAGCTC-3'; PTPN14-R: 5'-CCCTGTGCTTCCACCGAC-3'; GAPDH-F: 5'-GGGAAACTGTGGCGTGAT-3'; GAPDH-R: 5'-GAGTGGGT-GTCGCTGTTGA-3'; U6-F: 5'-CTCGCTTCGCGCAGCACA-3'; U6-R: 5'-AACGCTTCACGAATTTGCGT-3'.

Cell viability assay

Cells (3×10^3) were seeded into 96-well plates and stimulated with gradient concentrations of doxorubicin for 48 h. In addition, the corresponding cells (3×10^3) were cultured in 96-well plates for 0, 24, 48, or 72 h. Next, the cells were exposed to 3-(4,5-dimethyl-2-thiazolyl)-2,5-diphenyl-2-H-tetrazolium bromide (MTT) solution (Solarbio) for 2 h. Subsequently, dimethyl sulfoxide (DMSO; Solarbio) was added to each well. Finally, the optical density was measured at 490 nm using a Multi-Mode Reader (BioTek, Burlington, VT, USA). When cell viability was reduced to 50%, the corresponding doxorubicin concentration was defined as the half-maximal inhibitory concentration (IC₅₀).

Transwell assay

For cell migration assay, cells were injected into the upper chamber. Meanwhile, 10% FBS was added to the lower chamber. Then, the migrated cells were stained with crystal violet for 20 min. Subsequently, the cells were counted using a microscope in five randomly selected fields. For cell invasion assay, transwell chambers were coated with Matrigel (BD Biosciences, San Diego, CA, USA), with the remaining steps the same as those in the migration assay.

Western blot assay

Cells were lysed using RIPA buffer (Solarbio). Protein samples were separated by polyacrylamide gel electrophoresis and transferred onto polyvinylidene fluoride membranes (Millipore, Billerica, MA, USA). Next, the membranes were treated with primary antibodies against matrix metalloproteinase 9 (MMP9; ab38898, Abcam, Cambridge, UK), matrix metalloproteinase 2 (MMP2; ab97779, Abcam), CD63 (ab68418, Abcam), CD9 (ab223052, Abcam), PTPN14 (ab204321, Abcam), or GAPDH (ab9485, Abcam). Then, the membranes were probed with secondary antibody (ab7090, Abcam) for 2 h at room temperature. The protein bands were visualized using an enhanced chemiluminescence system (Qiagen).

Dual-luciferase reporter assay

CircPRRX1 or PTPN14 3'UTR containing miR-3064-5p wild-type or mutant binding sites was cloned into pmirGLO vector (Promega, Madison, WI, USA), named as circPRRX1 WT, circPRRX1 MUT, PTPN14 3'UTR WT, or PTPN14 3'UTR MUT.

Then, the constructed luciferase reporter and miR-3064-5p or miR-NC were co-transfected into HGC-27 and AGS cells. The luciferase activity was examined using the Dual-Lucy Assay Kit (Solarbio).

Xenograft assay

Xenograft experiments were approved by the Animal Research Committee of First Hospital of Shanxi Medical University. Briefly, lentiviral vectors harboring circPRRX1 short hairpin RNA (sh-circPRRX1) or control (sh-NC) were purchased from GenePharma. HGC-27/DR cells (5×10^6) transfected with sh-circPRRX1 or sh-NC were subcutaneously injected into the right backs of BALB/c nude mice ($n=7$ per group). After 5 days, the mice were given 5 mg/kg of doxorubicin every 5 days. Tumor volume was measured every 5 days. After 30 days, the xenograft was excised and weighed. Also, the expression levels of circPRRX1, miR-3064-5p, and PTPN14 were examined by qRT-PCR or Western blot.

Statistical analysis

GraphPad Prism 7.0 software (GraphPad, San Diego, CA, USA) was utilized to analyze all data. Data are presented as means \pm standard deviations. Differences were assessed using Student's t-test or one-way analysis of variance. $p < 0.05$ was considered statistically significant.

RESULTS

CircPRRX1 up-regulated in doxorubicin-resistant GC cells

To explore the regulatory effect of doxorubicin resistance, we treated parental cells (HGC-27 and AGS) with doxorubicin to construct doxorubicin-resistant cells (HGC-27/DR and AGS/DR). As exhibited in Fig. 1A and B, the IC₅₀ of doxorubicin in HGC-27/DR and AGS/DR cells was significantly higher than that in HGC-27 and AGS cells, indicating that doxorubicin-resistant cells were successfully established. Also, MTT analysis revealed that the proliferation ability of doxorubicin-resistant cells was markedly greater than that of parental cells (Fig. 1C and D). Furthermore, transwell assay demonstrated that doxorubicin-resistant cells exhibit increased cell migration and invasion relative to HGC-27 and AGS cells (Fig. 1E and F). Similarly, Western blot assay revealed marked elevations in EMT-related protein levels (MMP9 and MMP2), compared with parental cells (Fig. 1G and H). Moreover, heatmaps indicated the up-regulation of 18 circRNAs in GC tissues, and qRT-PCR showed that circPRRX1 expression was significantly increased in HGC-27/DR and AGS/DR cells, compared to parental cells (Fig. 1I, J, and K).

CircPRRX1 knockdown hinders GC progression and doxorubicin resistance in doxorubicin-resistant GC cells

Based on the abnormal up-regulation of circPRRX1 in doxorubicin-resistant GC cells, we used a series of loss-of-function experiments to test the relationship between circPRRX1 and doxorubicin resistance. First, the knockdown efficiency of circPRRX1 in doxorubicin-resistant cells was determined using qRT-PCR (Fig. 2A and B). Compared with the control group, circPRRX1 silencing reduced IC50 values in HGC-27/DR and AGS/DR cells (Fig. 2C and D). In addition, down-regulation of circPRRX1 suppressed the proliferation, migration, and invasion of HGC-27/DR and AGS/DR cells, compared to the control group (Fig. 2E-H). Also, Western blot analysis demonstrated that transfection with si-circPRRX1 resulted in a significant reduction in the levels of MMP9 and MMP2 (Fig. 2I and J). These data indicated that knockdown of circPRRX1 inhibits the cell viability, migration, and invasion of doxorubicin-resistant GC cells.

Extracellular circPRRX1 is packaged into exosomes

To determine whether circPRRX1 is secreted by exosomes, we examined the expression of circPRRX1 after treatment with RNase A or RNase A+Triton X100. The results revealed that circPRRX1 expression in the medium was not affected by RNase A, but was remarkably decreased after RNase A and Triton X100 treatment, indicating that circPRRX1 is enveloped by membranes rather than directly secreted (Fig. 3A). Next, we isolated exosomes from the culture medium of doxorubicin-resistant cells, and the representative images of exosomes were acquired by TEM (Fig. 3B). Additionally, Western blot analysis revealed the presence of exosome markers (CD63 and CD9) (Fig. 3C). Also, the expression of circPRRX1 in exosomes of doxorubicin-resistant cells was significantly higher than that in exosomes of parental cells (Fig. 3D). These data indicated that circPRRX1 is secreted by being transferred into exosomes.

Exosome-mediated circPRRX1 enhances doxorubicin resistance in GC cells

To investigate the effect of exosome-carried circPRRX1 on

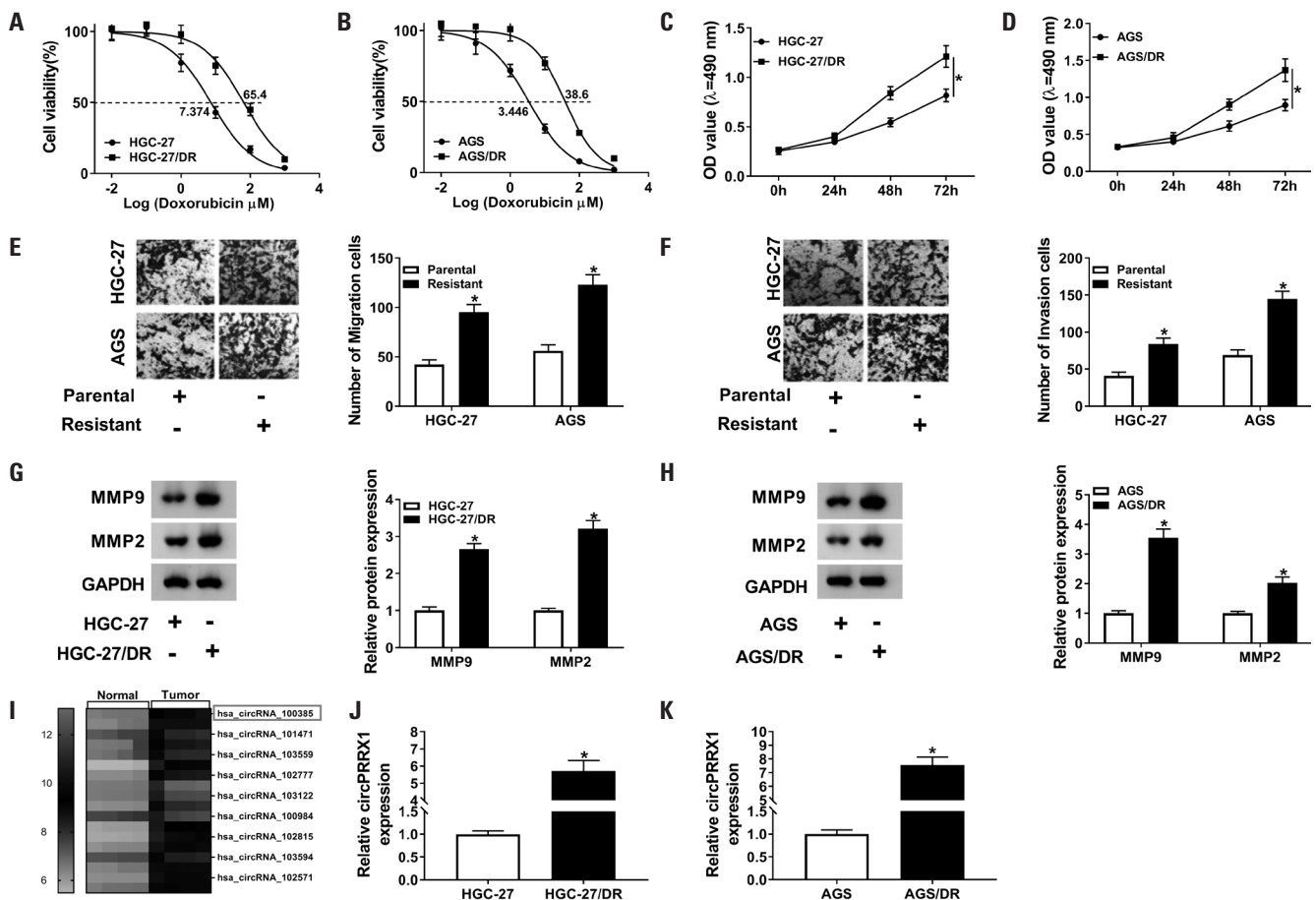


Fig. 1. CircPRRX1 is up-regulated in DR GC cell lines. (A and B) HGC-27, AGS, HGC-27/DR, and AGS/DR cells were treated with gradient concentrations of doxorubicin, and cell viability was detected by the MTT method. (C and D) Cell proliferation was assessed by MTT assay. (E and F) Cell migration and invasion were detected by transwell assay. (G and H) The levels of MMP9 and MMP2 were measured by Western blot. (I) A heatmap displays 18 circRNAs up-regulated in GC tissues. (J and K) The expression of circPRRX1 in parental cells (HGC-27 and AGS) and resistant cells (HGC-27/DR and AGS/DR) was examined by qRT-PCR. * $p < 0.05$. DR, doxorubicin-resistant; GC, gastric cancer.

doxorubicin resistance, HGC-27 and AGS cells were incubated with extracted exosomes before transfection with si-NC or si-circPRRX1. First, qRT-PCR showed a significant increase in circ-

cPRRX1 expression in recipient cells (HGC-27 and AGS) incubated with exosomes, suggesting that exosome-packaged circPRRX1 could be absorbed by recipient cells, whereas

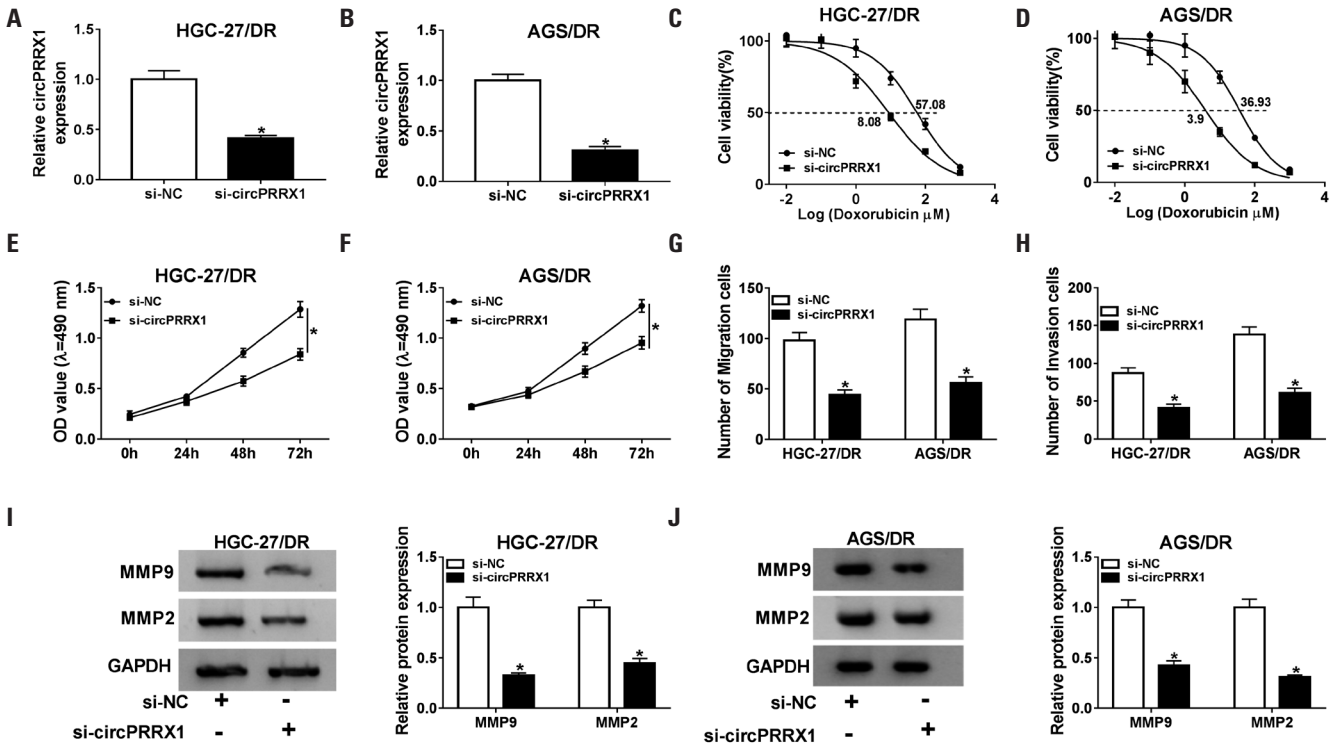


Fig. 2. CircPRRX1 knockdown hinders GC progression and doxorubicin resistance in DR-resistant GC cells. HGC-27/DR and AGS/DR cells were incubated with si-NC or si-circPRRX1. (A and B) The expression levels of circPRRX1 were measured using qRT-PCR. (C and D) After DR treatment, cell viability was examined by MTT assay and IC50 values were calculated. (E and F) Cell proliferation was evaluated by MTT assay. (G and H) Cell migration and invasion were measured by transwell assay. (I and J) The protein levels of MMP9 and MMP2 were detected by Western blot. * $p < 0.05$. DR, doxorubicin-resistant; GC, gastric cancer.

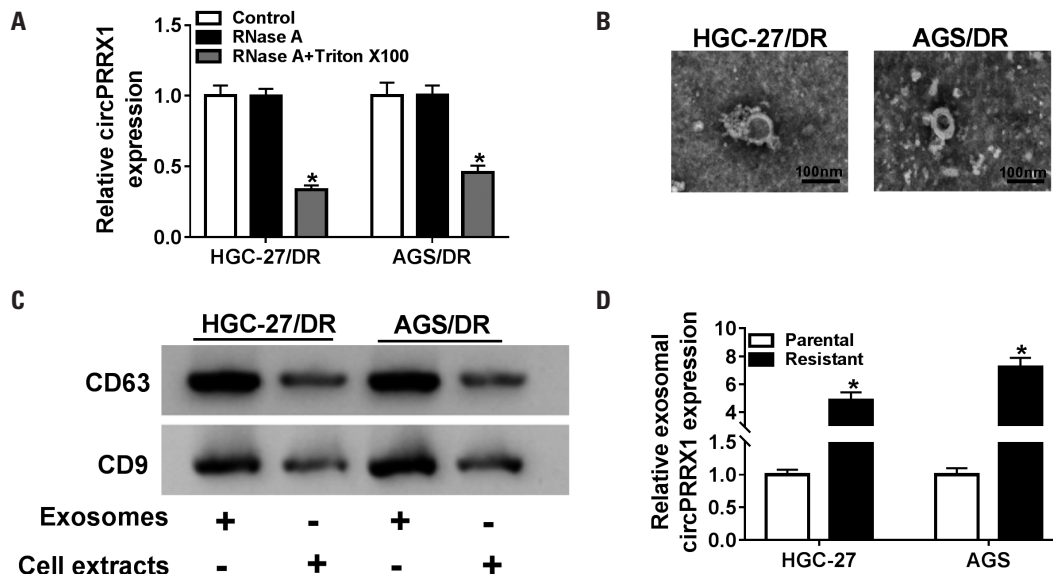


Fig. 3. Extracellular circPRRX1 is packaged into exosomes. (A) HGC-27/DR and AGS/DR cells were treated with 1 μ g/mL of RNase A alone or combined with 0.1% Triton \times 100 for 30 min, and circPRRX1 expression was detected using qRT-PCR. (B) Representative images of exosomes released by GC cells under a transmission electron microscope. (C) Exosome markers (CD63 and CD9) were detected by Western blot in purified exosomes and cell extracts. (D) The expression of circPRRX1 in exosomes of parental and resistant GC cells was measured by qRT-PCR. * $p < 0.05$. DR, doxorubicin-resistant; GC, gastric cancer.

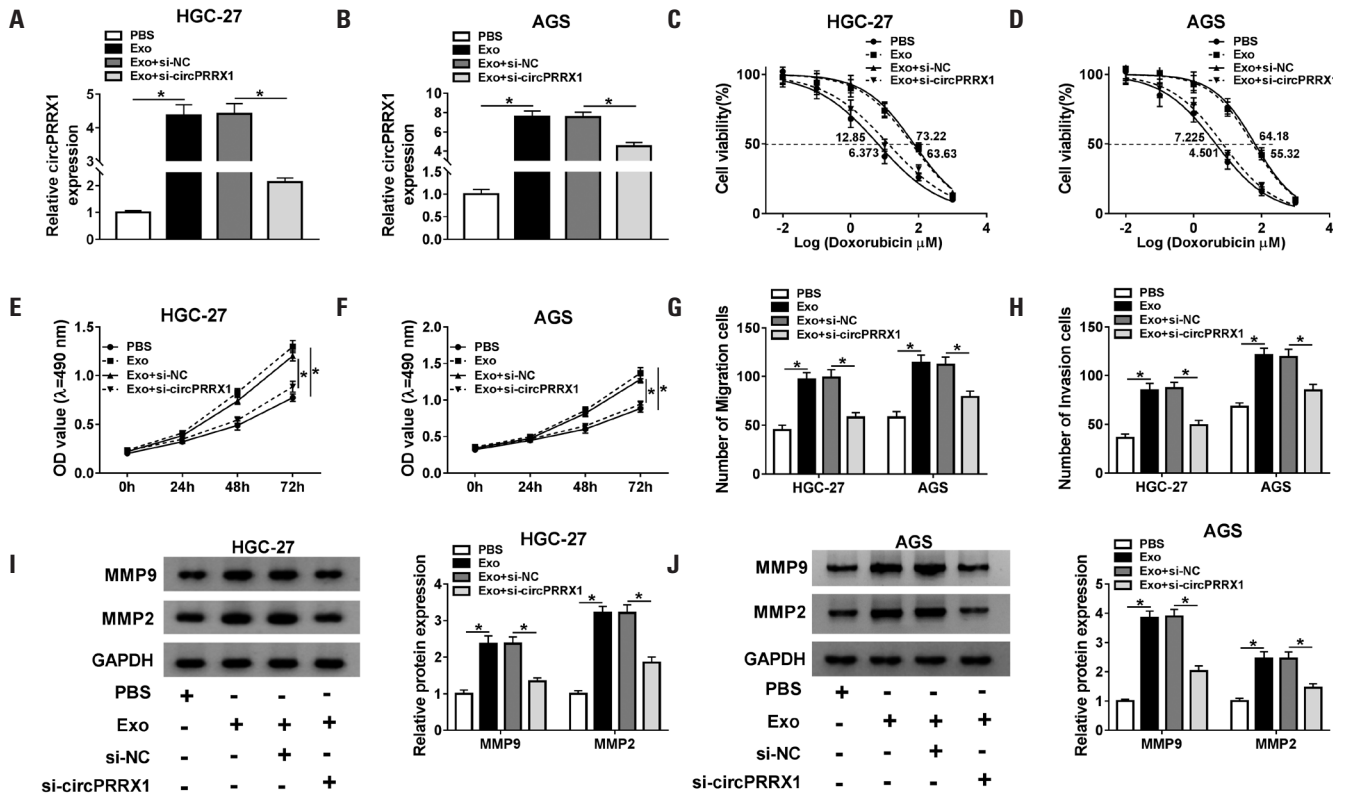


Fig. 4. Exosome-mediated circPRRX1 enhances doxorubicin resistance in GC cells. HGC-27 and AGS cells treated with extracted exosomes were transfected with si-NC or si-circPRRX1. PBS treatment was administered as a blank control. (A and B) circPRRX1 levels were detected by qRT-PCR. (C and D) MTT assay was used to detect cell viability and calculate IC50 values after doxorubicin stimulation. (E and F) MTT analysis was utilized to assess cell proliferation. (G and H) Transwell assay was conducted to detect the number of migrated and invaded cells. (I and J) Western blot assay was performed to measure MMP9 and MMP2 expression. * $p < 0.05$. GC, gastric cancer.

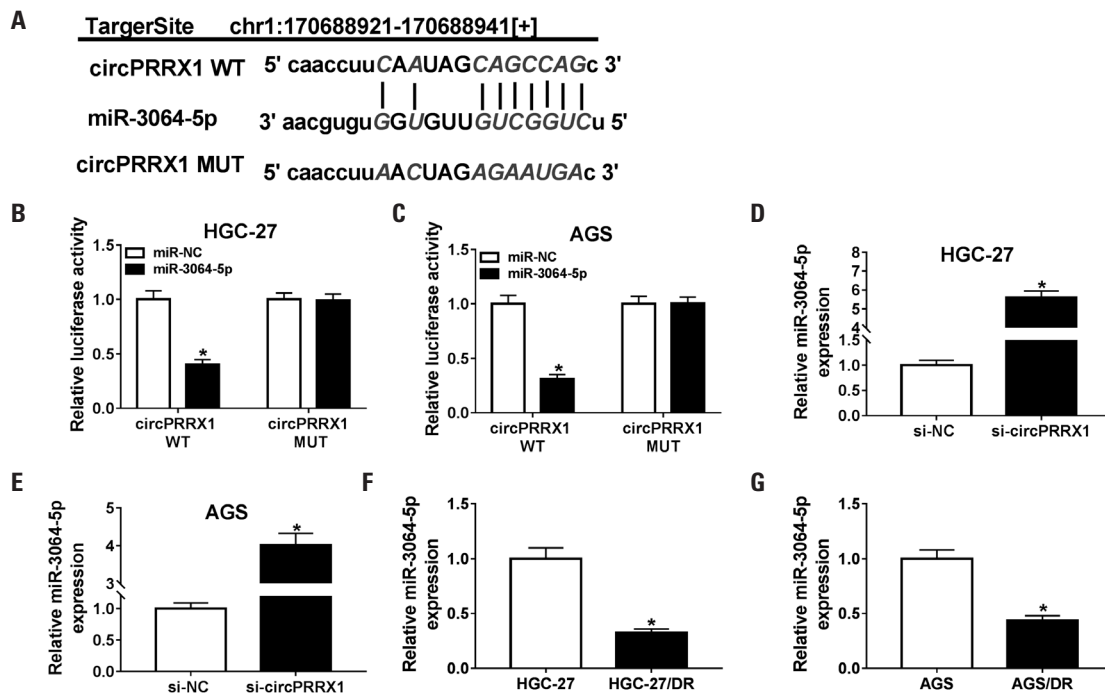


Fig. 5. CircPRRX1 directly interacts with miR-3064-5p. (A) The predicted binding sites of circPRRX1 and miR-3064-5p are shown. (B and C) HGC-27 and AGS cells were co-transfected with circPRRX1 WT or circPRRX1 MUT and miR-3064-5p or miR-NC, and luciferase activity was detected by dual-luciferase reporter assay. (D and E) miR-3064-5p expression was examined in HGC-27 and AGS cells transfected with si-NC or si-circPRRX1. (F and G) miR-3064-5p levels were measured in HGC-27, HGC-27/DR, AGS and AGS/DR cells. * $p < 0.05$. DR, doxorubicin-resistant.

transfection with si-circPRRX1 attenuated the up-regulation of circPRRX1 (Fig. 4A and B). Further, exosome treatment increased the IC50 values of HGC-27 and AGS cells, while inhibition of circPRRX1 abolished this effect (Fig. 4C and D). MTT analysis and transwell assay suggested that exosome incubation triggered cell proliferation, migration, and invasion in recipient cells, whereas these effects were abrogated by down-regulating circPRRX1 (Fig. 4E-H). Furthermore, silencing of circPRRX1 reversed the elevation in MMP9 and MMP2 expression stimulated by exosome treatment (Fig. 4I and J).

CircPRRX1 directly interacts with miR-3064-5p

The putative binding site of circPRRX1 and miR-3064-5p was predicted by starBase v2.0 database (Fig. 5A). Dual-luciferase reporter assay revealed that miR-3064-5p mimics strikingly reduced the luciferase activity of circPRRX1 WT reporter (Fig. 5B and C). Next, HGC-27 and AGS cells were transfected with si-

NC or si-circPRRX1, and qRT-PCR showed that knockdown of circPRRX1 remarkably increased the expression levels of miR-3064-5p (Fig. 5D and E). Meanwhile, miR-3064-5p levels were markedly decreased in HGC-27/DR and AGS/DR cells, compared with HGC-27 and AGS cells (Fig. 5F and G). Collectively, these data showed that circPRRX1 directly targets miR-3064-5p.

Inhibition of miR-3064-5p reverses the effect of circPRRX1 depletion on doxorubicin-resistant GC cells

First, knockdown of circPRRX1 abolished the down-regulation of miR-3064-5p induced by HGC-27 and AGS cells incubated with exosomes (Fig. 6A and B). To further investigate whether circPRRX1 affected doxorubicin resistance by regulating miR-3064-5p, a series of functional rescue experiments were performed in doxorubicin-resistant cells. The results of qRT-PCR suggested that transfection with anti-miR-3064-5p

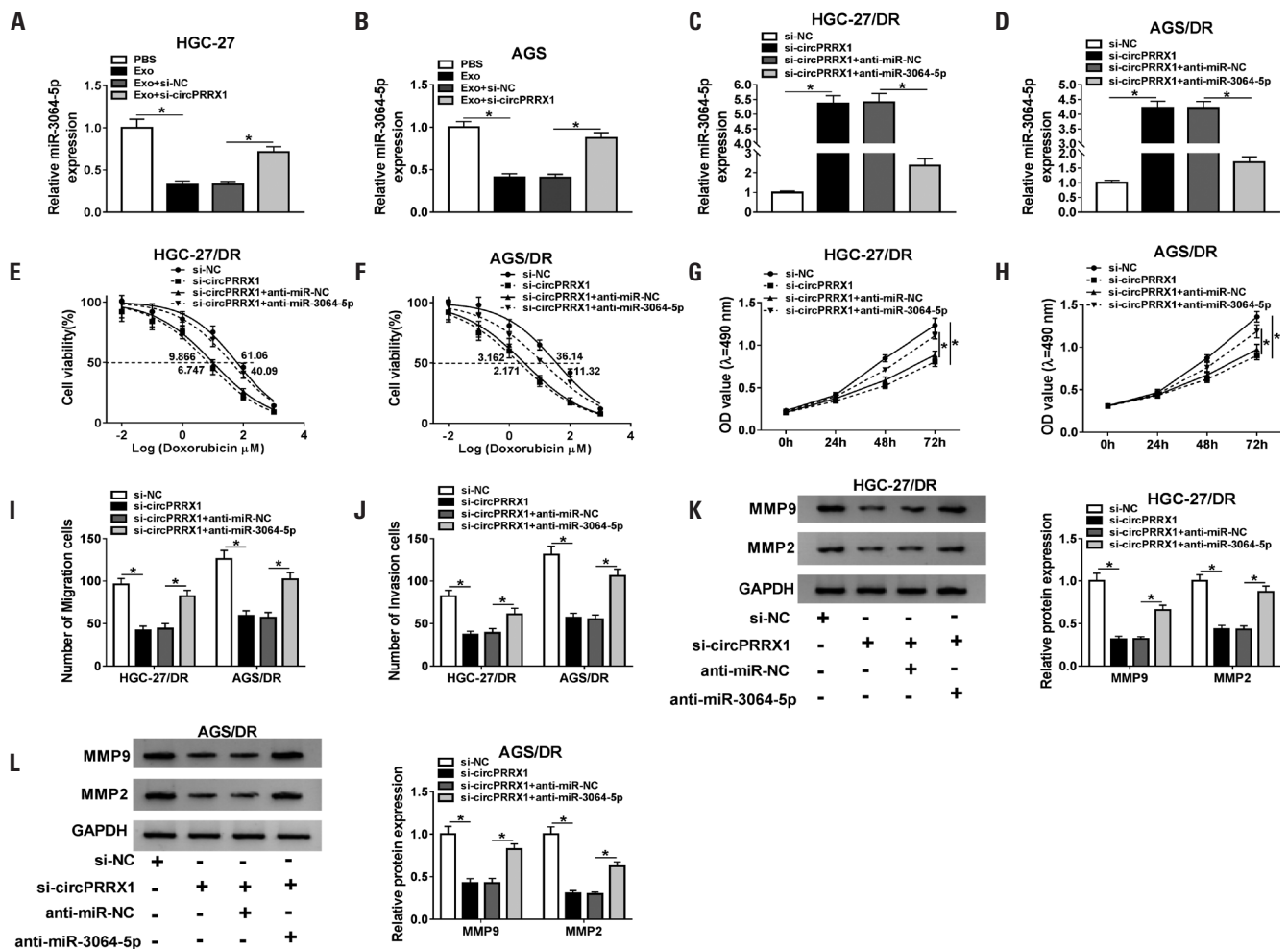


Fig. 6. Inhibition of miR-3064-5p reverses the effect of circPRRX1 depletion on DR-resistant GC cells. (A and B) HGC-27 and AGS cells treated with exosomes were incubated with si-NC or si-circPRRX1, and miR-3064-5p expression was measured using qRT-PCR. (C-L) HGC-27/DR and AGS/DR cells were transfected with si-NC, si-circPRRX1, si-circPRRX1+anti-miR-NC, or si-circPRRX1+anti-miR-3064-5p, respectively. (C and D) The expression levels of miR-3064-5p were detected by qRT-PCR. (E and F) After treatment with different doses of doxorubicin, cell viability was measured by MTT assay, and IC50 values were calculated. (G and H) Cell proliferation was evaluated by MTT assay. (I and J) Cell migration and invasion were detected by transwell assay. (K and L) The levels of MMP9 and MMP2 were measured by Western blot. **p*<0.05. DR, doxorubicin-resistant; GC, gastric cancer.

alleviated the increases in miR-3064-5p expression caused by circPRRX1 knockdown (Fig. 6C and D). Moreover, inhibition of circPRRX1 impeded cell proliferation, migration, and invasion in doxorubicin-resistant cells, while miR-3064-5p inhibitor reversed these effects (Fig. 6E-J). Also, introduction of anti-miR-3064-5p abrogated the reduced expression of MMP9 and MMP2 induced by down-regulation of circPRRX1 (Fig. 6K and L). These data indicated that circPRRX1 depletion suppresses cell proliferation, migration, and invasion by modulating miR-3064-5p in doxorubicin-resistant GC cells.

PTPN14 is targeted by miR-3064-5p

To further elucidate the mechanism of circPRRX1 in GC, we again employed the starBase v2.0 database, which predicted that PTPN14 may be a potential target of miR-3064-5p (Fig. 7A). Then, dual-luciferase reporter assay was performed in HGC-27 and AGS cells co-transfected with PTPN14 3'UTR WT or PTPN14 3'UTR MUT and miR-3064-5p or miR-NC. The results demonstrated that mature miR-3064-5p significantly decreases the luciferase activity of WT-TRIM44 reporter (Fig. 7B and C). In addition, PTPN14 protein levels in HGC-27/DR and AGS/DR cells were markedly higher than those in HGC-27 and AGS cells (Fig. 7D and E). Overexpression of

miR-3064-5p inhibited PTPN14 protein expression in HGC-27 and AGS cells (Fig. 7F and G). Furthermore, suppression of circPRRX1 overtly reduced PTPN14 protein levels, whereas miR-3064-5p inhibitor rescued the effect (Fig. 7H and I). These data suggested that circPRRX1 regulates PTPN14 expression by sponging miR-3064-5p.

PTPN14 overexpression reverses the effect of circPRRX1 knockdown on resistant GC cells

Next, we performed a series of rescue experiments to investigate whether circPRRX1 regulates doxorubicin resistance by affecting PTPN14. As exhibited in Fig. 8A and B, silencing of circPRRX1 abrogated increased PTPN14 expression in HGC-27 and AGS cells elicited by exosome treatment. Additionally, transfection with PTPN14 undermined the down-regulation of PTPN14 expression caused by circPRRX1 depletion (Fig. 8C and D). Furthermore, circPRRX1 knockdown suppressed cell proliferation, migration, and invasion in doxorubicin-resistant cells, whereas the effects were overturned by overexpressing PTPN14 (Fig. 8E-J). At the same time, up-regulation of PTPN14 alleviated the decrease in MMP9 and MMP2 expression caused by circPRRX1 inhibition (Fig. 8K and L). These data indicated that circPRRX1 silencing repressed cell proliferation,

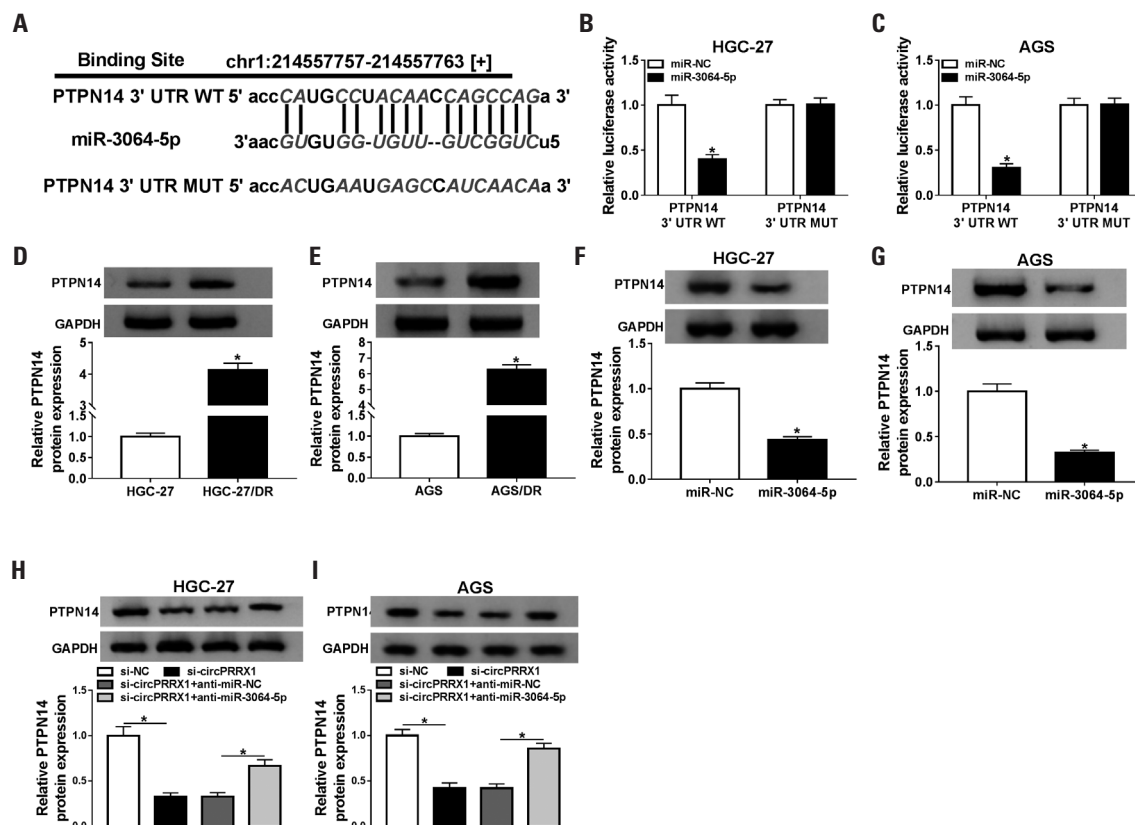


Fig. 7. PTPN14, a target of miR-3064-5p. (A) The putative binding sites for miR-3064-5p and PTPN14 3'UTR are displayed. (B and C) The targeting relationship between miR-3064-5p and PTPN14 was verified by dual-luciferase reporter assay. (D and E) The protein levels of PTPN14 in HGC-27, HGC-27/DR, AGS and AGS/DR cells were examined using Western blot. (F and G) PTPN14 protein expression was detected in HGC-27 and AGS cells transfected with miR-NC or miR-3064-5p. (H and I) PTPN14 protein levels were measured in HGC-27 and AGS cells transfected with si-NC, si-circPRRX1, si-circPRRX1+anti-miR-NC, or si-circPRRX1+anti-miR-3064-5p. * $p < 0.05$. DR, doxorubicin-resistant.

migration, and invasion by regulating PTPN14 in doxorubicin-resistant GC cells.

Serum exosomal circPRRX1 is associated with doxorubicin resistance in GC patients

Exosomes were extracted from the serum of 56 GC patients treated with doxorubicin, and qRT-PCR showed that circPRRX1 expression was significantly higher in patients who did not respond to doxorubicin than in patients who responded to doxorubicin (Fig. 9A). To clarify the stability of circPRRX1 in serum exosomes, the extracted exosomes were incubated at different times, treated with RNase A, or cultured with solutions of different pH values. Then, circPRRX1 expression was detected after

treatment with different conditions, and the results revealed that circPRRX1 levels were not affected by any experimental conditions (Fig. 9B-D). Meanwhile, receiver operating characteristic curves demonstrated that exosomal circPRRX1 had a high diagnostic value for GC patients (Fig. 9E). In addition, the proportion of patients who responded to doxorubicin treatment in the high circPRRX1 expression group was significantly lower than that in the low circPRRX1 expression group (Fig. 9F). These data suggested that exosomal circPRRX1 could be used as a diagnostic biomarker for GC patients.

CircPRRX1 enhances doxorubicin resistance in vivo

To investigate the effect of circPRRX1 on doxorubicin resis-

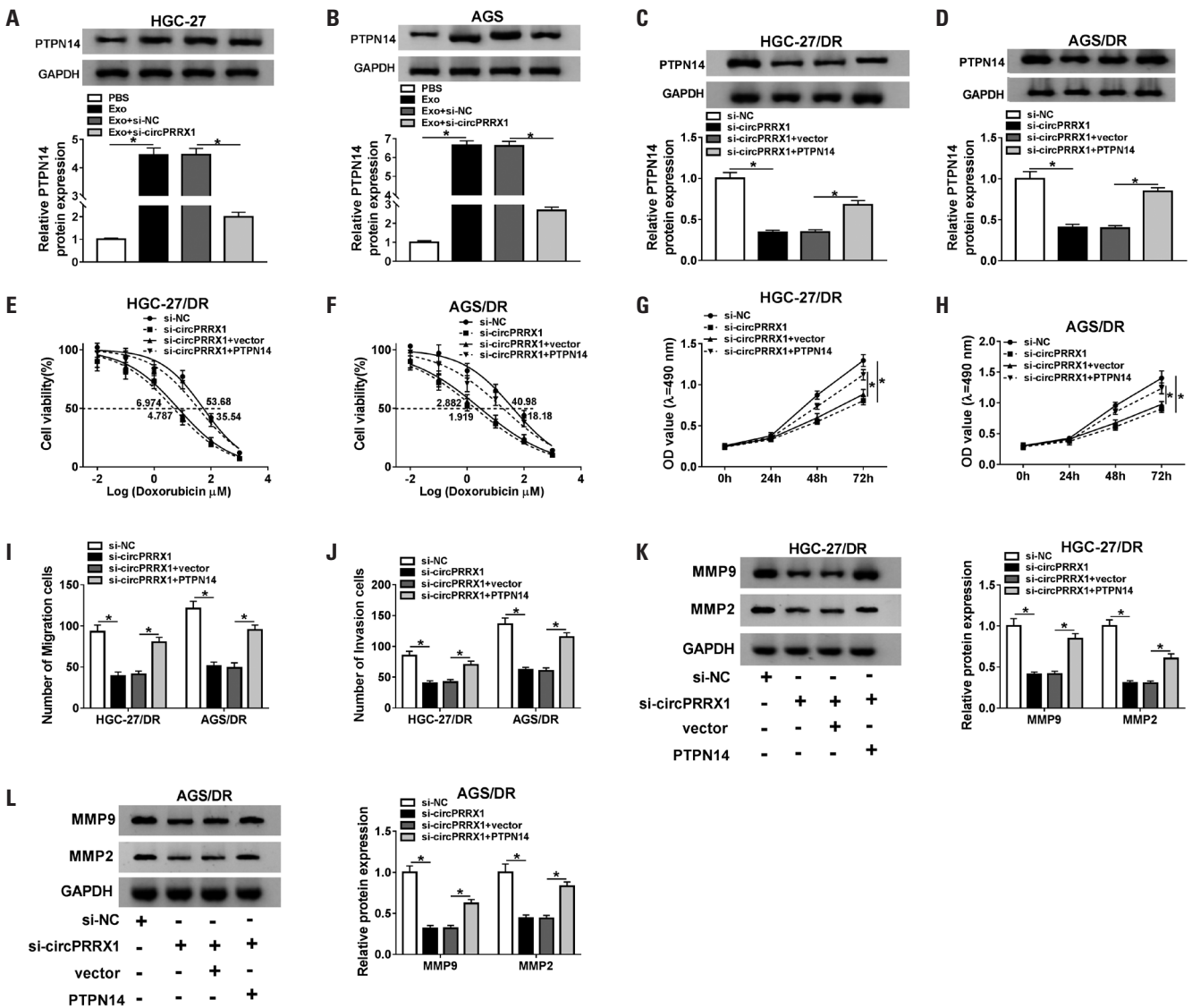


Fig. 8. PTPN14 overexpression reverses the effect of circPRRX1 knockdown in resistant GC cells. (A and B) HGC-27 and AGS cells were transfected with si-NC or si-circPRRX1 after incubation with exosomes, and the protein levels of PTPN14 were detected using Western blot. (C-L) HGC-27/DR and AGS/DR cells were transduced with si-NC, si-circPRRX1, si-circPRRX1+vector, or si-circPRRX1+PTPN14, respectively. (C and D) The expression of PTPN14 was measured by Western blot. (E and F) Cell viability was determined by the MTT method, and IC50 values were calculated. (G and H) MTT assay was used to assess cell proliferation. (I and J) Transwell assay was utilized to detect cell migration and invasion. (K and L) The protein levels of MMP9 and MMP2 were measured by Western blot assay. * p <0.05. DR, doxorubicin-resistant; GC, gastric cancer.

tance in vivo, a xenograft model was established by subcutaneously injecting HGC-27/DR cells transfected with sh-NC or sh-circPRRX1 into nude mice. After 5 days, mice were dosed with doxorubicin every 5 days. The results illustrated that circPRRX1 silencing and doxorubicin stimulation remarkably reduced tumor volume and weight, compared to doxorubicin treatment

alone (Fig. 10A and B). After treatment with doxorubicin, transfection with sh-circPRRX1 decreased the levels of circPRRX1 and PTPN14 and increased miR-3064-5p expression (Fig. 10C-E). These results indicated that silencing of circPRRX1 reduces doxorubicin resistance in vivo.

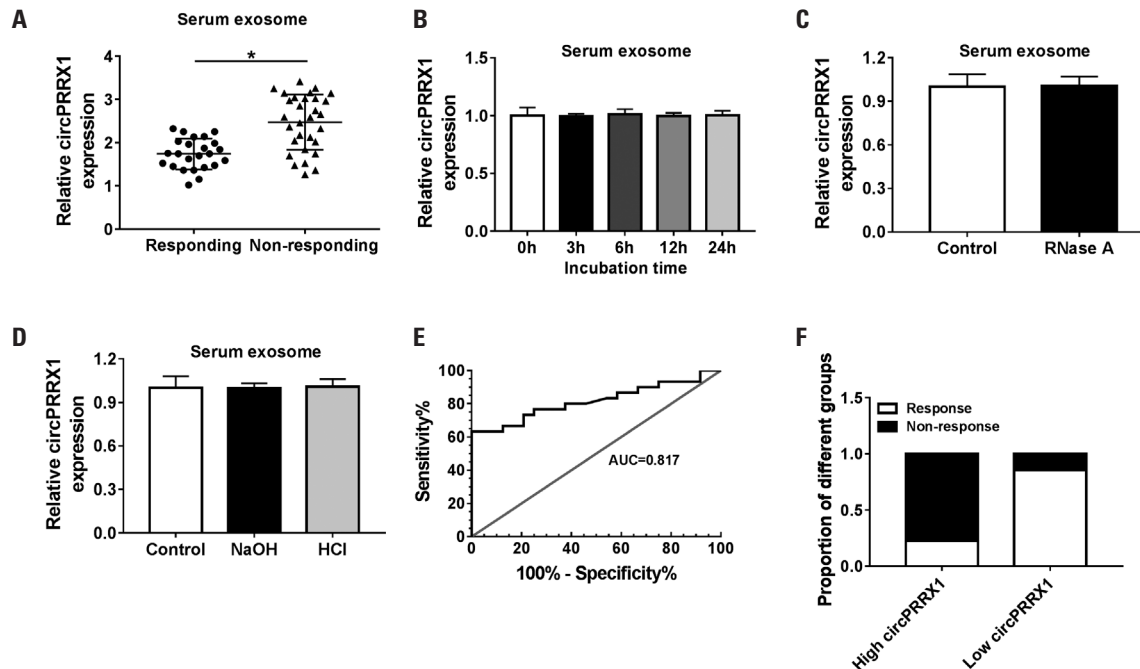


Fig. 9. Serum exosomal circPRRX1 is associated with doxorubicin resistance in GC patients. (A) Serum exosomes were extracted from GC patients responding or not responding to doxorubicin treatment, and circPRRX1 expression was detected using qRT-PCR. (B) The expression of circPRRX1 was detected after serum exosomes were incubated for different times. (C) CircPRRX1 expression was measured after serum exosomes were treated with RNase A. (D) CircPRRX1 expression was examined after serum exosomes were stimulated with NaOH or HCl. (E) The diagnostic value of exosomal circPRRX1 in GC patients treated with doxorubicin was analyzed by ROC curves. (F) The proportions of patients resistant to doxorubicin treatment in high circPRRX1 expression and low circPRRX1 expression groups are shown. * $p < 0.05$. GC, gastric cancer.

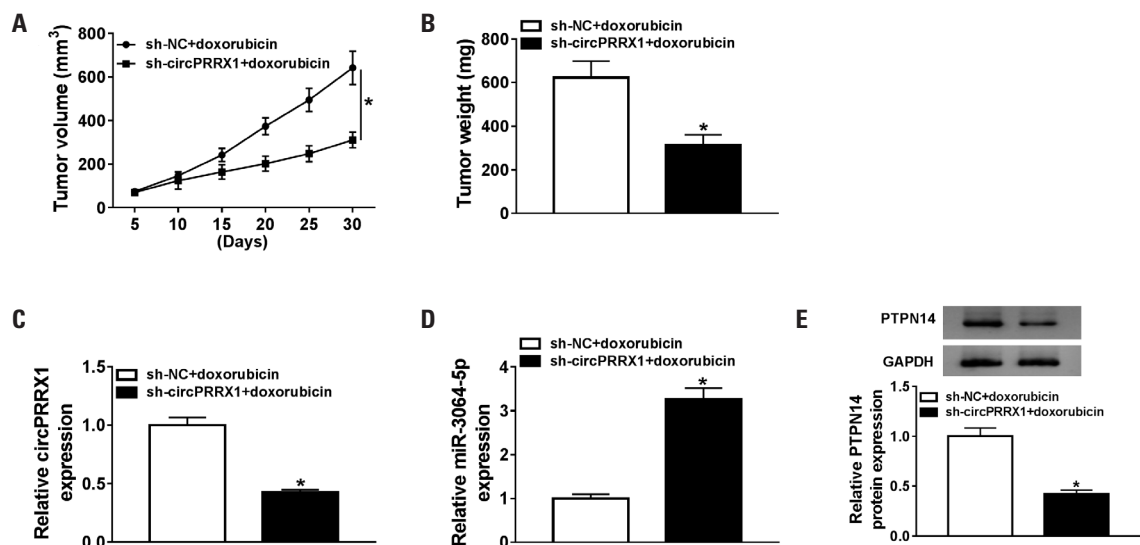


Fig. 10. CircPRRX1 enhances doxorubicin resistance in vivo. HGC-27/DR cells transfected with sh-NC or sh-circPRRX1 were subcutaneously injected into the right backs of nude mice. (A) After 5 days, the mice were given 5 mg/kg of doxorubicin every 5 days, and the tumor volume was measured. (B) The mice were killed 30 days later, and the tumors were weighed. (C and D) The levels of circPRRX1 and miR-3064-5p were measured by qRT-PCR. (E) The protein expression of PTPN14 was detected by Western blot. * $p < 0.05$.

DISCUSSION

The emergence of chemoresistance has become a major stumbling block in the treatment of advanced GC.^{16,17} The molecular mechanisms of drug resistance are complex, and non-coding RNAs play a critical role in mediating chemoresistance in tumors.¹⁸ In addition, tumor-derived exosomes modulate tumor metastasis, angiogenesis, and chemoresistance.¹⁹ In the current study, we clarified the relationship between exosome-mediated circPRRX1 and doxorubicin resistance in GC.

Mounting evidence suggests that circRNAs play a regulatory role in a range of biological functions through the ceRNA mechanism.^{20,21} For example, Huang, et al.²² discovered that circAKT3 potentiates cisplatin resistance in GC via functioning as a ceRNA. A through inhibition of miR-198 and up-regulation PIK3R1. Ma, et al.²³ revealed that circRACGAP1 enhances resistance to apatinib in GC cells through modulation of autophagy via regulating a miR-3657/ATG7 pathway. Furthermore, research has revealed that circPRRX1 expedites the development of esophageal cancer by binding to miR-1294 and up-regulating LASP1.²⁴ Based on the significant up-regulation of circPRRX1 expression in GC, we speculated that circPRRX1 plays a carcinogenic role in GC. Loss-of-function experiments showed that knockdown of circPRRX1 reduces the malignancy of GC and doxorubicin resistance.

In this study, we discovered that circPRRX1 is secreted by exosomes and that exosomal circPRRX1 increases doxorubicin resistance. Studies have indicated that circRNAs are enriched and stable in exosomes and that exosomal circRNAs are important mediators of intercellular communication.²⁵ In terms of mechanisms, circPRRX1 was a decoy for miR-3064-5p. In hepatocellular carcinoma, miR-3064-5p blocked angiogenesis by binding to MALAT1 and regulating the FOXA1 pathway.²⁶ In GC, circCOL6A3 was found to facilitate tumor progression by acting as a sponge for miR-3064-5p and activating COL6A3.²⁷ In our research, miR-3064-5p was down-regulated in doxorubicin-resistant cells. Interestingly, inhibition of miR-3064-5p reversed the effect of circPRRX1 silencing on doxorubicin resistance and tumor progression.

We also speculated that circPRRX1 regulated PTPN14 expression by serving as a sponge for miR-3064-5p. Han, et al.²⁸ suggested that PTPN14 aggravates the malignancy of GC via regulating YAP phosphorylation. Wang, et al.²⁹ demonstrated that HOTAIR increases PTPN14 expression to improve GC cell resistance to paclitaxel and doxorubicin by sponging miR-217. In the present study, PTPN14 was overtly up-regulated in doxorubicin-resistant cells. Furtherly, PTPN14 overexpression rescued the effect of circPRRX1 depletion on doxorubicin sensitivity and cell growth and metastasis.

Since exosomal circPRRX1 could be transferred to sensitive cells to develop doxorubicin resistance, we further examined the level of circPRRX1 in serum exosomes. In recent years, studies have corroborated that circRNAs in serum exosomes

are abundant and stable, making them a tumor detection factor and a promising biomarker for tumor diagnosis and prognosis.³⁰ We found that exosomal circPRRX1 could serve as a diagnostic biomarker for GC patients.

In conclusion, we first confirmed that exosome-transferred circPRRX1 induces doxorubicin resistance and suppresses cell growth and metastasis in doxorubicin resistant-GC cells. In clinical chemotherapy, exosomal circPRRX1 in serum may be a promising diagnostic biomarker for patients with GC.

AUTHOR CONTRIBUTIONS

Conceptualization: Bin Song. **Data curation:** Mei Ping and Bin Song. **Formal analysis:** Shumin Wang and Mei Ping. **Investigation:** Shumin Wang. **Methodology:** Shumin Wang, Mei Ping, and Bin Song. **Project administration:** Mei Ping. **Resources:** Shumin Wang and Mei Ping. **Software:** Bin Song and Yarong Guo. **Supervision:** Yuanfei Li and Junmei Jia. **Validation:** Yarong Guo and Junmei Jia. **Visualization:** Yuanfei Li. **Writing—original draft:** Shumin Wang. **Writing—review & editing:** Shumin Wang. **Approval of final manuscript:** all authors.

ORCID iDs

Shumin Wang	https://orcid.org/0000-0003-0543-2331
Mei Ping	https://orcid.org/0000-0003-1339-4363
Bin Song	https://orcid.org/0000-0002-0333-8379
Yarong Guo	https://orcid.org/0000-0002-1506-546X
Yuanfei Li	https://orcid.org/0000-0002-9219-6914
Junmei Jia	https://orcid.org/0000-0002-9835-0636

REFERENCES

- Bray F, Ferlay J, Soerjomataram I, Siegel RL, Torre LA, Jemal A. Global cancer statistics 2018: GLOBOCAN estimates of incidence and mortality worldwide for 36 cancers in 185 countries. *CA Cancer J Clin* 2018;68:394-424.
- Amieva M, Peek RM Jr. Pathobiology of helicobacter pylori-induced gastric cancer. *Gastroenterology* 2016;150:64-78.
- Biagioni A, Skalamera I, Peri S, Schiavone N, Cianchi F, Giommoni E, et al. Update on gastric cancer treatments and gene therapies. *Cancer Metastasis Rev* 2019;38:537-48.
- Su M, Xiao Y, Ma J, Tang Y, Tian B, Zhang Y, et al. Circular RNAs in cancer: emerging functions in hallmarks, stemness, resistance and roles as potential biomarkers. *Mol Cancer* 2019;18:90.
- Tang X, Zhu J, Liu Y, Chen C, Liu T, Liu J. Current understanding of circular RNAs in gastric cancer. *Cancer Manag Res* 2019;11:10509-21.
- Lu J, Wang YH, Yoon C, Huang XY, Xu Y, Xie JW, et al. Circular RNA circ-RanGAP1 regulates VEGFA expression by targeting miR-877-3p to facilitate gastric cancer invasion and metastasis. *Cancer Lett* 2020;471:38-48.
- Liu YY, Zhang LY, Du WZ. Circular RNA circ-PVT1 contributes to paclitaxel resistance of gastric cancer cells through the regulation of ZEB1 expression by sponging miR-124-3p. *Biosci Rep* 2019;39:BSR20193045.
- Huang XX, Zhang Q, Hu H, Jin Y, Zeng AL, Xia YB, et al. A novel circular RNA circFN1 enhances cisplatin resistance in gastric cancer via sponging miR-182-5p. *J Cell Biochem* 2020.
- Cui X, Wang J, Guo Z, Li M, Li M, Liu S, et al. Emerging function

- and potential diagnostic value of circular RNAs in cancer. *Mol Cancer* 2018;17:123.
10. Liu X, Yang N, Figel SA, Wilson KE, Morrison CD, Gelman IH, et al. PTPN14 interacts with and negatively regulates the oncogenic function of YAP. *Oncogene* 2013;32:1266-73.
 11. Liang G, Duan C, He J, Ma W, Dai X. PTPN14, a target gene of miR-4295, restricts the growth and invasion of osteosarcoma cells through inactivation of YAP1 signalling. *Clin Exp Pharmacol Physiol* 2020;47:1301-10.
 12. Liu YP, Sun XH, Cao XL, Jiang WW, Wang XX, Zhang YF, et al. MicroRNA-217 suppressed epithelial-to-mesenchymal transition in gastric cancer metastasis through targeting PTPN14. *Eur Rev Med Pharmacol Sci* 2017;21:1759-67.
 13. Tran PHL, Xiang D, Tran TTD, Yin W, Zhang Y, Kong L, et al. Exosomes and nanoengineering: a match made for precision therapeutics. *Adv Mater* 2020;32:e1904040.
 14. Meldolesi J. Exosomes and ectosomes in intercellular communication. *Curr Biol* 2018;28:R435-44.
 15. Shi X, Wang B, Feng X, Xu Y, Lu K, Sun M. circRNAs and exosomes: a mysterious frontier for human cancer. *Mol Ther Nucleic Acids* 2020;19:384-92.
 16. Park DJ, Lenz HJ. Determinants of chemosensitivity in gastric cancer. *Curr Opin Pharmacol* 2006;6:337-44.
 17. Marin JJ, Al-Abdulla R, Lozano E, Briz O, Bujanda L, Banales JM, et al. Mechanisms of resistance to chemotherapy in gastric cancer. *Anticancer Agents Med Chem* 2016;16:318-34.
 18. Zhang X, Xie K, Zhou H, Wu Y, Li C, Liu Y, et al. Role of non-coding RNAs and RNA modifiers in cancer therapy resistance. *Mol Cancer* 2020;19:47.
 19. Mashouri L, Yousefi H, Aref AR, Ahadi AM, Molaei F, Alahari SK. Exosomes: composition, biogenesis, and mechanisms in cancer metastasis and drug resistance. *Mol Cancer* 2019;18:75.
 20. Zhong Y, Du Y, Yang X, Mo Y, Fan C, Xiong F, et al. Circular RNAs function as ceRNAs to regulate and control human cancer progression. *Mol Cancer* 2018;17:79.
 21. Qu S, Liu Z, Yang X, Zhou J, Yu H, Zhang R, et al. The emerging functions and roles of circular RNAs in cancer. *Cancer Lett* 2018;414:301-9.
 22. Huang X, Li Z, Zhang Q, Wang W, Li B, Wang L, et al. Circular RNA AKT3 upregulates PIK3R1 to enhance cisplatin resistance in gastric cancer via miR-198 suppression. *Mol Cancer* 2019;18:71.
 23. Ma L, Wang Z, Xie M, Quan Y, Zhu W, Yang F, et al. Silencing of circRACGAP1 sensitizes gastric cancer cells to apatinib via modulating autophagy by targeting miR-3657 and ATG7. *Cell Death Dis* 2020;11:169.
 24. Zhang Z, Lin W, Gao L, Chen K, Yang C, Zhuang L, et al. Hsa_circ_0004370 promotes esophageal cancer progression through miR-1294/LASP1 pathway. *Biosci Rep* 2019;39:BSR20182377.
 25. Wang Y, Liu J, Ma J, Sun T, Zhou Q, Wang W, et al. Exosomal circRNAs: biogenesis, effect and application in human diseases. *Mol Cancer* 2019;18:116.
 26. Zhang P, Ha M, Li L, Huang X, Liu C. MicroRNA-3064-5p sponged by MALAT1 suppresses angiogenesis in human hepatocellular carcinoma by targeting the FOXA1/CD24/Src pathway. *FASEB J* 2020;34:66-81.
 27. Sun X, Zhang X, Zhai H, Zhang D, Ma S. A circular RNA derived from COL6A3 functions as a ceRNA in gastric cancer development. *Biochem Biophys Res Commun* 2019;515:16-23.
 28. Han X, Sun T, Hong J, Wei R, Dong Y, Huang D, et al. Nonreceptor tyrosine phosphatase 14 promotes proliferation and migration through regulating phosphorylation of YAP of Hippo signaling pathway in gastric cancer cells. *J Cell Biochem* 2019;120:17723-30.
 29. Wang H, Qin R, Guan A, Yao Y, Huang Y, Jia H, et al. HOTAIR enhanced paclitaxel and doxorubicin resistance in gastric cancer cells partly through inhibiting miR-217 expression. *J Cell Biochem* 2018;119:7226-34.
 30. Fanale D, Taverna S, Russo A, Bazan V. Circular RNA in exosomes. *Adv Exp Med Biol* 2018;1087:109-17.